

# Spectral statistics of multi-parametric Gaussian ensembles with chiral symmetry

Triparna Mondal and Pragya Shukla

*Department of Physics, Indian Institute of Technology,*

*Kharagpur-721302, West Bengal, India*

(Dated: September 15, 2022)

## Abstract

The statistics of chiral matrix ensembles with uncorrelated but multivariate Gaussian distributed elements is intuitively expected to be driven by many parameters. Contrary to intuition, however, our theoretical analysis reveals the existence of a single parameter, a function of all ensemble parameters, which governs the dynamics of spectral statistics. The analysis not only extends the similar formulation (known as complexity parameter formulation) for the Hermitian ensembles without chirality to those with it but also reveals the underlying connection between chiral complex systems with seemingly different system conditions as well as to other complex systems e.g. multi-parametric Wishart ensembles as well as generalized Calogero Sutherland Hamiltonian (CSH).

## I. INTRODUCTION

For systems in which the relevant behavior is governed by a linear operator, it is useful to consider the matrix-representation in a symmetry preserving basis which in turn puts the constraints on the type of matrix elements and/or structure of the matrix [1–3] (referred as matrix constraints). The underlying complexity in real systems however often manifests through fluctuations of physical properties making it necessary to consider their statistical behavior [4–6]. This in turn requires an analysis of not only a single matrix but rather their ensemble, with latter's choice sensitive to the system specific conditions e.g. hopping range, dimensionality, boundary conditions etc; the conditions on the choice of ensemble i.e its parameters as well as nature of randomness is referred as ensemble constraints. The latter can conspire with matrix constraints in multiple ways to give rise to different types of statistical behavior. This motivates the present study in which the primary focus is to analyze the influence of a specific *matrix constraint*, namely chiral symmetry, on the statistical behavior of complex systems with varying *ensemble constraints* e.g disorder [2]. The motivation comes not only from the fundamental aspect of the topic but also from a range of applications in which complexity appears hand in hand with chirality e.g. charge transport in graphene [7], spectral fluctuations in QCD Dirac operators [8, 9], conductance fluctuations in mesoscopic systems [1, 10], topological systems etc [11–14].

Consider a complex system with chiral symmetry described by an ensemble of chiral Hermitian matrices. For special cases in which the complexity subjects the matrix elements to independent and identical distributions (e.g. cases with ergodic dynamics in the basis space) thus resulting in minimum number of ensemble constraints, the system can then be represented by a basis-invariant chiral ensemble e.g chiral Gaussian ensemble invariant under orthogonal, unitary or symplectic transformation (referred as Ch-GOE, Ch-GUE and Ch-GSE respectively) [4–6, 8]. For generic cases however the information about inhomogeneity of system conditions appears through ensemble parameters (e.g. those with localized dynamics in basis space), and as a consequence an appropriate ensemble representation depends on many of them. Any variation of the system conditions changes the ensemble parameters, thus leading to a multi-parametric evolution of the matrix ensemble (in a fixed basis) and it is

natural to wonder whether any universality classes can be identified during non-equilibrium stages. As revealed by previous studies, the answer is in affirmative at least in the case of the multi-parametric, non-chiral, Hermitian ensembles (of real-symmetric, complex Hermitian or real quaternion matrices); the reasoning is based on a common mathematical formulation of their statistical properties in which ensemble details enter only through a single function of all distribution parameters. Using the function, referred as the complexity parameter, the non-chiral ensembles can be mapped to a single parametric Brownian ensemble of corresponding symmetry-class (real, complex Hermitian or real-quaternion) [15–20]. The latter can be described as an ensemble of Hermitian matrices  $H = H_0 + \sqrt{Y} V$ , with  $H_0$  taken from one of the stationary ensemble of Hermitian matrices, subjected to perturbation  $V$  taken from another stationary ensemble and  $Y$  as the perturbation parameter [21, 23, 24]. The mapping not only reveals the underlying universality among non-equilibrium (non-stationary or basis-dependent) Hermitian ensembles but also helps the application of all available information for the latter to former. A similar formulation in case of chiral Hermitian matrices is very desirable as well as intuitively expected but is not technically obvious; this is because their off-diagonal blocks are in general non-Hermitian. This motivates us to analyze the multi-parametric Gaussian ensembles of chiral Hermitian matrices with and without time-reversal symmetry and seek a single parametric formulation of their spectral and strength (i.e eigenfunctions) fluctuations. As discussed later, the diffusion equation for the ensemble density (joint probability density function of the matrix elements) in terms of the complexity parameter turns out to be analogous to that of a chiral Brownian ensemble (Ch-BE), a perturbed stationary chiral ensemble with its diffusion governed by the perturbation parameter[25]; a direct diagonalization of the diffusion equation then leads to analogous diffusion equations for the spectral as well as strength statistical measures. Some of the fluctuations measures for the Ch-BE are theoretically analyzed in [25], with their formulation expressed in terms of perturbation parameter. By replacing the latter by the complexity parameter, the information can then directly be used for the multi-parametric Gaussian ensembles of chiral Hermitian matrices.

The implications of the single parametric formulation of the statistics for the multi-parametric chiral ensembles are many e.g. it reveals (i) analogy among the statistics of different complex systems, represented by the ensembles of different ensemble constraints but same matrix constraints, (ii) analogy of the statistics of a complex system for different

system conditions, (iii) the connection to a variant of Calogero-Sutherland Hamiltonian (CSH) thus providing further evidence supporting the claim that the CSH is hidden backbone Hamiltonian of the world of complex systems [26], (iii) the possibility of a similar formulation for multi-parametric Wishart ensembles. The importance of these connections as well as the implications makes it necessary to verify our theoretical predictions and is primary focus of the present work. For this purpose, we numerically analyze the spectral statistics of the four Gaussian chiral ensembles with different functional dependence of the distribution parameters.

The paper is organized as follows. The section II describes the diffusion of the multi-parametric probability density of the chiral ensemble under consideration and presents the complexity parametric formulation of its diffusion when the ensemble parameters (a few or all) are varied. As the steps are essentially the same as in non-chiral case discussed in [16], we avoid repeatiton here and only mention the diffusion equation for the ensemble density. An exact diagonalization of the latter then leads to complexity parameter driven diffusion equations for the joint probability distribution functions of the eigenvalues and eigenfunctions. The relevant steps are described in section III; here again we mention only those steps which are different from the non-chiral cases. The numerical analysis presented in section IV verifies our theoretical predictions. The connections of chiral ensembles with some other complex systems is described in section V. We conclude in section VI with a brief summary of our results and open questions.

## II. MULTI-PARAMETRIC GAUSSIAN ENSEMBLES WITH CHIRALITY AND HERMITIAN CONSTRAINTS

### A. Matrix-representation

A  $(2N + \nu) \times (2N + \nu)$  Hermitian matrix with chirality constraint can be described as

$$H = \begin{pmatrix} 0 & C \\ C^\dagger & 0 \end{pmatrix}. \quad (1)$$

where  $C$  is a general a  $N \times (N + \nu)$  complex matrix if  $H$  has no other anti-unitary symmetry; as clear from above,  $H_{k,N+l} = C_{kl}$ . For cases with time-reversal symmetry also present,  $C$  is a real or quaternion matrix based on the presence/ absence of rotational symmetry (i.e

integer or half integer angular momentum). For clarity purposes, here we confine our study only to  $C$  real or complex with no other matrix constraints. The elements of  $C$  matrix can then be written as  $C_{kl} = \sum_{s=1}^{\beta} (i)^{s-1} C_{kl;s}$  where  $k = 1 \rightarrow N, l = 1 \rightarrow (N + \nu)$  and  $\beta = 1$  or  $2$  for  $C$  real or complex. (The generalization to quaternion  $C$  can be done following similar steps but is technically tedious and is therefore not included here).

## B. Diffusion of matrix elements: ensemble complexity parameter

Using eq.(1), the distribution, say  $\rho(H)$ , of the elements of the matrix  $H$  can be expressed in terms of those of  $C$ :

$$\rho(H) = \rho_c(C) F_c F_h \quad (2)$$

with  $\rho_c(C)$  as the probability density of the ensemble of  $C$  matrices, with  $F_h$  and  $F_c$  as the constraints due to Hermiticity and chirality of  $H$ , respectively:  $F_h(H) = \delta(H - H^\dagger)$  and  $F_c = \prod_{k,l=1}^N \delta(H_{kl})$

For simple presentation of our formulation, here we consider elements of  $C$  as independent Gaussian distributed, with arbitrary mean and variances:

$$\rho_c(C; h, b) = \mathcal{N} \exp \left[ - \sum_{k,l,s} \frac{1}{2h_{kl;s}} (C_{kl;s} - b_{kl;s})^2 \right] \quad (3)$$

with  $\sum_{k,l,s} \equiv \sum_{k=1}^N \sum_{l=1}^{N+\nu} \sum_{s=1}^{\beta}$  and  $\mathcal{N}$  as a normalization constant. Here  $h \equiv [h_{kl;s}]$  and  $b \equiv [b_{kl;s}]$  refer to the matrices of variances and mean values of  $C_{kl;s}$ . Clearly, with different choices of  $h$  and  $b$ -matrices, eq.(3) can give rise to many chiral ensembles; some of them are used later in section VI for numerical verification of our results.

Using  $H_{k,N+l} = C_{kl}$ , eq.(3) leads to the ensemble density  $\rho(H)$  of the  $H$ - matrix

$$\rho(H; h, b) = \mathcal{N} \exp \left[ - \sum_{k,l,s} \frac{1}{2h_{kl;s}} (H_{k(N+l)} - b_{kl;s})^2 \right] F_c F_h \quad (4)$$

We now consider a diffusive dynamics in the ensemble-space of  $C$ -matrices by a smooth variation of the parameters  $h_{kl;s}$  and  $b_{kl;s}$ . As the dynamics occurs in  $C$ -matrix space, it preserves the chirality of  $H$ . Proceeding as discussed in [17, 19], the single parametric evolution of the  $\rho_c(C)$  can now be described as

$$\frac{\partial \rho_c}{\partial Y} = \sum_{k,l,s} \frac{\partial}{\partial C_{kl;s}} \left[ \frac{\partial \rho_c}{\partial C_{kl;s}} + \gamma C_{kl;s} \rho_c \right] \quad (5)$$

where  $Y$  is referred as the ensemble complexity parameter:

$$Y = -\frac{1}{2M\gamma} \ln \left[ \prod_{k,l;s} |1 - 2\gamma h_{kl;s}| |b_{kl;s}|^2 \right] + \text{const} \quad (6)$$

with  $M = 2N + \nu$ . Substitution of  $C_{kl;s} = H_{kN+l;s}$  in the above then leads to the evolution equation for  $\rho(H)$

$$\frac{\partial \rho}{\partial Y} = \sum_{k,l,s} \frac{\partial}{\partial H_{kN+l;s}} \left[ \frac{\partial \rho}{\partial H_{kN+l;s}} + \gamma H_{kN+l;s} \rho \right] \quad (7)$$

The above equation describes the diffusion of  $\rho(H)$  with a finite drift, starting from an arbitrary initial condition, say  $\rho_0(H, Y_0)$  at  $Y = Y_0$ . As the system information in the above equation enters only through  $Y$ , its solution  $\rho(H)$  remains same for different ensembles, irrespective of the details of  $h$  and  $b$  matrices, if they share same  $Y$ -value and are subjected to same global constraints; the latter ensures the existence of a common initial state for them.

As in the non-chiral case [15], an exact diagonalization of eq.(7) leads to the diffusion equations for the eigenvalues and eigenfunctions. In this paper, we confine the discussion to the spectral statistics only. The approach however requires a prior information about the response of the eigenvalues and eigenfunctions to the variation of  $H_{kl;s}$  which differ for the two cases. As the steps for the derivation of diffusion equations are analogous to non-chiral case, the next section states only the final results.

### III. SPECTRAL STATISTICS

#### A. Spectral response to change in system conditions

With  $H$  given by eq.(1), let  $E$  be its eigenvalue matrix ( $E_{mn} = e_n \delta_{mn}$ ) and  $U$  as the eigenvector matrix, with  $U_{kn}$  as the  $k^{\text{th}}$  component of the eigenvector  $U_n$  corresponding to eigenvalue  $e_n$ . Following from eq.(1),  $\text{Tr}(H)$  is zero which then implies that the eigenvalues of  $H$  exist in equal and opposite pairs or are zero; let us refer such pairs as  $e_n, e_{n+N}$  with  $e_n = -e_{n+N}$ ,  $1 \leq n \leq N$ . Clearly, with  $E$  as  $(2N + \nu) \times (2N + \nu)$  diagonal matrix, the number of zero eigenvalues is  $\nu$ . Henceforth, the eigenvalues are labelled such that  $e_k$ ,  $k = 1 \rightarrow N$  correspond to positive eigenvalues with their negative counterparts lying from  $k = N + 1 \rightarrow 2N$  and  $k = 2N + 1 \rightarrow 2N + \nu$  refers to zero eigenvalues.

A variation of system conditions perturbs  $H$  which in turn change  $E$  and  $U$ . The latter's response to change in  $H$  can be derived from the eigenvalue equation  $HU = UE$  along with the unitary condition  $U^\dagger U = I_{2N+\nu}$  (as discussed in [15] for the non-chiral case). With our focus in spectral statistics only, here we describe only the spectral responses. Assuming, the

variation of system conditions leaves the chirality of  $H$  unaffected, the eigenvalues  $e_{2N+k}$  for  $k = 1 \rightarrow \nu$  therefore remain zero throughout the dynamics. The dynamics of  $e_n$ , with  $n = 1 \rightarrow N$ , can then be given as

$$\frac{\partial e_n}{\partial H_{k,N+l;s}} = i^{s-1} [U_{kn}^* U_{N+l,n} + (-1)^{s+1} U_{N+l,n}^* U_{kn}] \quad (8)$$

The above in turn gives

$$\sum_{k,l=1}^{N,N+\nu} \sum_{s=1}^{\beta} \frac{\partial e_n}{\partial H_{k,N+l;s}} H_{k,N+l;s} = e_n \quad (9)$$

Further

$$\sum_{k,l=1}^{N,N+\nu} \sum_{s=1}^{\beta} \frac{\partial e_n}{\partial H_{k,N+l;s}} \frac{\partial e_m}{\partial H_{k,N+l;s}} = \beta \delta_{mn} \quad 1 \leq m, n \leq N \quad (10)$$

$$\sum_{k,l=1}^{N,N+\nu} \sum_{s=1}^{\beta} \frac{\partial^2 e_n}{\partial H_{k,N+l;s}^2} = \frac{\beta(\nu + 1/2)}{e_n} + \sum_{m=1 \neq n}^N \frac{2\beta e_n}{e_n^2 - e_m^2} \quad (11)$$

As expected the replacement  $e_n \rightarrow -e_{N+n}$  leaves the eq.(8, 9, 10,11) invariant; (note as discussed in [25], chirality leads to the condition  $U_{N+l,N+n} = -U_{(N+l),n}$ ).

## B. Joint Probability distribution of eigenvalues

Let us define  $P(E) \equiv P(e_1, e_2, \dots, e_{2N+\nu})$  as the joint probability density function (JPDF) of the eigenvalues  $e_i$ ,  $i = 1, 2, \dots, 2N + \nu$  of  $H$ . Using eq.(5) along with relations (8,9,10,11) and proceeding exactly as described in [15, 17, 18] for the non-chiral cases, the  $Y$  governed evolution of  $P(E; Y)$  can be described as

$$\frac{\partial P}{\partial Y} = 2 \sum_{n=1}^N \frac{\partial}{\partial e_n} \left[ \frac{\partial}{\partial e_n} - \beta \left( \frac{\nu + 1/2}{e_n} + \sum_{m=1}^N \frac{2e_n}{e_n^2 - e_m^2} \right) + \gamma e_n \right] P \quad (12)$$

The above equation describes the diffusion of  $P(E, Y)$  due to variation of  $Y$  from an arbitrary initial state  $P(E_0, Y_0)$  at  $Y = Y_0$ . In limit  $\frac{\partial P}{\partial Y} \rightarrow 0$  or  $Y \rightarrow \infty$ , the diffusion approaches a unique steady state:  $P(E; \infty) = C_\beta |Q_N|^\beta$  with  $C_\beta$  as the normalization constant and

$$|Q_N|^\beta = \prod_{m < n=1}^N |e_m^2 - e_n^2|^\beta \prod_{k=1}^N |e_k|^{\nu\beta + \beta - 1} e^{-\frac{\gamma}{2} \sum_{k=1}^N e_k^2} \quad (13)$$

Eq.(12) can also be derived by an alternative but more illuminating route. This follows by noting that eq.(7) is analogous to the diffusion equation for the ensemble density of a chiral Brownian ensemble (ChBE). An exact diagonalization of both the equations is therefore expected to lead to an analogous diffusion equation for  $P(E, Y)$  which is indeed the case (see [25]). The theoretical results, obtained in [25]), for the statistics of chiral Brownian

ensembles can then directly be used for the multi-parametric chiral Gaussian ensembles. For example, the spectral correlations of the latter can then be described by eq.(1) of [25] with  $Y$  given by eq.(6).

### C. Fluctuation measures

The  $Y$ -based formulation of the spectral JPDF given by eq.(12) indicates its applicability to a wide range of chiral ensembles. But as discussed in [25], the evolution of a spectral fluctuation measure depends on a rescaled complexity parameter

$$\Lambda_e(Y, e) = \frac{(Y - Y_0)}{\Delta_{loc}^2}. \quad (14)$$

with  $\Delta_{loc}$  as the local mean level spacing. The rescaling is needed to compare the local fluctuations imposed on different spectral density backgrounds. As discussed in [25],  $\Lambda_e$  is the only parameter (besides energy range of interest) which appears in the differential equations determining the local spectral fluctuations; the latter will be same for two different ensembles if (i) both have same  $\Lambda_e$  value, and, (ii) both evolve from an analogous initial condition (statistically). To verify the prediction, we pursue a numerical comparison of different chiral ensembles illustrated in next section.

*Local mean level spacing:* As clear from eq.(14), a determination of  $\Lambda_e$  requires a prior knowledge of  $Y - Y_0$  as well as  $\Delta_e$ . While  $Y$  is explicitly given by eq.(6), the formulation of  $\Delta_{loc}$  depends on the underlying eigenfunction dynamics; for the eigenfunctions with non-ergodic dynamics, it can be significantly different from the mean level spacing  $\Delta(e)$ . This can be explained as follows: while  $\Delta_{loc}(e)$  corresponds to only those levels at energy  $e$  which are occupying the same region in basis space,  $\Delta(e)$  refers to all levels at energy  $e$  irrespective of their location in the basis-space. (This is because levels with eigenfunctions localized in different parts of basis space do not interact but  $\Delta(e)$  is obtained by taking into account all levels in the spectrum irrespective of their interaction). Based on the above reasoning, one possible definition can be given as follows:  $\Delta_{loc}(e) = \frac{1}{\langle \rho_{loc} \rangle}$  where

$$\rho_{loc}(e) = \sum_n \phi_n \delta(e - e_n) \quad (15)$$

with  $\phi_n$  as the probability of  $n^{th}$  eigenfunction occupying the same region as other eigenfunctions with energies close to  $e$ . For example, for the case in which a typical eigenfunction is delocalized in entire Hilbert space, the above implies  $\phi_n = 1$  which gives  $\langle \rho_{loc}(e) \rangle = R_1(e)$  and



$\Delta_{loc}(e) = \Delta(e)$ . Similarly, in the case of localized dynamics, although two localized states do not typically overlap but can be localized in the same region with a small probability of  $\xi^d/(2N)$  (with  $\xi(e)$  as the average localization radius at energy  $e$ ,  $d$  as the system-dimension and  $2N$  as the number of basis states). This implies  $\phi_n \sim \frac{\xi^d}{2N}$  which gives  $\rho_{loc}(e) = \frac{\xi^d}{2N} R_1(e)$ . Using  $R_1(e) = \frac{1}{\Delta(e)}$ , this leads to

$$\Delta_{loc}(e) = \Delta(e) \frac{2N}{\xi^d} \quad (16)$$

(with  $\xi^d/2N$  as the probability of eigenfunctions localized in the same region of basis space). For cases where the eigenfunctions are exponentially localized e.g. in standard Anderson Hamiltonian (a single particle moving in a random potential),  $\xi^d$  can be approximated by the average inverse participation ratio  $\langle I_2 \rangle$  of the eigenfunctions with energies  $\sim e$ :  $\xi^d \approx (\langle I_2 \rangle)^{-1}$ . The latter relation however is not valid in general and one has to use the alternate routes to determine  $\xi$ .

#### IV. NUMERICAL VERIFICATION OF SINGLE PARAMETRIC FORMULATION

Based on the complexity parametric formulation, different ensembles subjected to same global constraint (e.g Hermitian as well chiral nature of  $H$ -matrix in the present study) are expected to undergo similar evolution. This in turn implies an analogy of their spectral statistical measures if  $\Lambda_e$  (eq.(14) for them have same values and the initial conditions (at  $Y = Y_0$ ) are statistically analogous. In this section, we verify the analogy by numerically comparing the spectral fluctuations of four multi-parametric Gaussian ensembles of real-symmetric chiral matrices with different variance types. The determination of  $\Lambda_e$  however requires a prior knowledge of  $Y - Y_0$  as well as  $\Delta_e$  which depends on the ensemble-details as discussed below. The section also illustrates as to how different ensembles, if subjected to same matrix constraints, can be justified to evolve from same initial condition.

##### A. Details of the Ensembles

The ensembles can briefly be described as follows.

**Chiral Rosenzweig-Porter Ensemble (Ch-RPE):** This is a chiral variant of the standard Rosenzweig-Porter ensemble [21, 22], with  $\rho(H)$  given by eq.(4) where

$$h_{kk} = \langle C_{kk}^2 \rangle = 1, \quad h_{kl} = \langle C_{kl}^2 \rangle = \frac{1}{(1 + \mu)}, \quad k \neq l, \quad b_{kl} = \langle C_{kl} \rangle = 0 \quad (\forall k, l) \quad (17)$$

with  $0 < \mu < \infty$ ; the limits  $\mu = 0$  and  $\infty$  correspond to a chiral Gaussian orthogonal ensemble (Ch-GOE) and a matrix ensemble with diagonal chiral blocks, respectively. Substitution of the above values in eq.(6) gives  $Y$  for this case

$$Y = -\frac{N(N-1)}{2M\gamma} \ln \left[ 1 - \frac{2\gamma}{(1 + \mu)} \right] + c_0 \quad (18)$$

with  $M = N^2$  and  $c_0$  as a constant of integration (determined by the initial condition on the ensemble).

Choosing initial condition with  $\mu \rightarrow \infty$  corresponds to an ensemble of  $H$  matrices, with its chiral blocks as diagonal  $C$ -matrices and the spectral statistics as Poisson statistics (with chiral constraint). From eq.(18, this implies  $Y_0 = c_0$  and  $Y - Y_0 \approx \frac{1}{\mu}$  (for  $\mu \gg 1$ ). This on substitution in eq.(14) leads to the spectral complexity parameter for Ch-RPE case

$$\Lambda_{e,B}(e) = \frac{Y - Y_0}{\Delta_e(e)^2} \approx \frac{R_1^2}{\mu}. \quad (19)$$

Here the 2nd equality is obtained by using  $\Delta_e(e) = \frac{1}{R_1(e)}$ . As clear from the above,  $\Lambda_{e,B}$  depends on three parameters, namely,  $\mu$ , matrix size  $N$  as well as the spectral location  $e$  chosen for the analysis of the local fluctuations.

The ensemble density with distribution parameters given by eq.(17) is analogous to a specific class of chiral Brownian ensemble (Ch-BE) [25], namely, that arising due to a single parametric perturbation of a chiral ensemble, with Poisson statistics for non-zero eigenvalues, by a Ch-GOE ensemble; we henceforth refer the Ch-RPE case as Ch-BE case.

For numerical study of Ch-RPE, we choose the case with  $\mu = c N^2$ ; (the choice is motivated by previous studies of non-chiral Rosenzweig-Porter ensembles (or Brownian ensembles) which confirm this  $\mu$ -value as a critical point of the statistics [21]). The ensemble is exactly diagonalised for two different  $c$  values, i.e.  $c = 1$  and  $c = 0.4$ , each case considered for two different matrix-sizes  $2N = 1000$  and  $2N = 1728$ . The requires  $R_1$  to determine  $\Lambda_e$  in this case is obtained numerically.

**Chiral Anderson Ensemble (Ch-AE):** The  $H$ -matrix in this case represents the Hamiltonian, in a site basis, for a particle moving on a  $d$ -dimensional bipartite lattice with

an isotropic Gaussian hopping between nearest neighbours sites of two different sub-lattices. The diagonal disorder as well as the nearest neighbour hopping within an unit cell is assumed to be zero (thus implying  $H_{kk} = 0$ ). The ensemble density for this case can be described by eq.(3) with

$$h_{kk} = \langle C_{kk}^2 \rangle = w^2/12, \quad h_{kl} = \langle C_{kl}^2 \rangle = f_1 w_s^2/12, \quad b_{kl} = \langle C_{kl} \rangle = f_2 t \quad (20)$$

where  $f_1(kl) = 1, f_2(k, l) = 1$  for  $\{k, l\}$  pairs representing hopping,  $f_1(k, l), f_2(k, l) \rightarrow 0$  for all  $\{k, l\}$  values corresponding to disconnected sites. From eq.(6), the ensemble complexity parameter in this case is [16]

$$Y = -\frac{N}{2M\gamma} \ln [ |1 - \gamma w^2/6| |1 - \gamma w_s^2/6|^z |t + \delta_{t0}|^z ] + c_0 \quad (21)$$

where  $M$  and  $c_0$  same as in the previous case and  $zN$  as the number of nearest neighbours which depends on the lattice conditions as well as the dimensionality  $d$  of the system.

To determine  $Y_0$ , the initial state is chosen as a clean bipartite lattice with sufficiently far off atoms resulting in zero hopping (i.e both  $w = w_s = 0$ ); consequently the initial ensemble corresponds to a localized eigenfunction dynamics with Poisson spectral statistics (with chiral constraint) and  $Y_0 = c_0$ . Substitution of eq.(21) in eq.(14) with  $\Delta_e(e) = \frac{2N\langle I_2 \rangle}{R_1}$  and  $\overline{\langle I_2 \rangle}$  as the typical ensemble as well as spectral averaged inverse participation ratio (IPR) at  $e$ , leads to the spectral complexity parameter

$$\Lambda_{e,A}(Y, N, e) = \frac{R_1^2}{8\gamma N^3 \overline{\langle I_2 \rangle}^2} \ln [ |1 - \gamma w^2/6| |1 - \gamma w_s^2/6|^z |t + \delta_{t0}|^z ]. \quad (22)$$

For numerics of this case, we consider two Ch-AEs, each consisting of two dimensional lattices (with  $z = 4$ ), one of 5000 matrices of size  $2N = 1024$ , and, another 2500 matrices of  $2N = 2116$ ; each ensemble is analyzed for two disorder strength  $w^2 = 12$  and  $36$  (keeping  $w_s^2 = 12$  and  $t = 0$  for both cases). The required values of  $R_1$  and  $\langle I_2 \rangle$  to determine  $\Lambda_e$  in this case are obtained numerically.

**Chiral Gaussian ensemble with Power law decay (Ch-PE):** The  $C$ -matrix ensemble in this case consists of independently distributed Gaussian entries with zero mean and a power law decay of variances away from the diagonal. The ensemble density  $\rho(H)$  can again be described by eq.(4) with

$$h_{kl} = \langle C_{k,l}^2 \rangle = \frac{1}{1 + \frac{|k-l|^2}{b^2}}, \quad b_{kl} = \langle C_{kl} \rangle = 0 \quad \forall k, l \quad (23)$$

where  $b$  is arbitrary parameter. Eq.(6) then gives

$$Y = -\frac{1}{2M\gamma} \left[ 2 \sum_{r=0}^N (N-r) \ln \left( 1 - \frac{2\gamma}{1 + (r/b)^2} \right)^2 \right] + c_0 \quad (24)$$

with number of independent elements  $M = N^2$  and  $r \equiv |k-l|$ . Here the case  $b \ll 1$  corresponds to  $H$ -ensemble with diagonal  $C$ -matrices with Poisson spectral statistics and can therefore be chosen as the initial ensemble. The choice leads to  $Y_0 = c_0$ .

The above along with eq.(14), with  $\Delta_e(e) = \frac{2N\langle I_2 \rangle}{R_1}$  then leads to

$$\Lambda_{e,P}(b, e) = \frac{R_1^2}{8\gamma N^4 \langle I_2 \rangle^2} \left[ 2 \sum_{r=0}^N (N-r) \ln \left( 1 - \frac{2\gamma}{1 + (r/b)^2} \right)^2 \right] \quad (25)$$

The spectral statistics of Ch-PE therefore shows a crossover from Poisson (for  $\Lambda_{e,P} \rightarrow 0$  as  $b \rightarrow 0$ ) to Chiral GOE behavior (for  $\Lambda_{e,P} \rightarrow \infty$  as  $b \rightarrow \infty$ ).

The numerics in this case is considered for an ensemble of 5000 matrices of size  $2N = 1000$  and another of 2500 matrices of size  $2N = 2000$ ; each ensemble is analyzed for two  $b$ -values i.e  $b = 0.25$  and  $0.15$ . Here again the  $\Lambda_e$  is determined by numerically obtained values of  $R_1$  and  $\langle I_2 \rangle$ .

**Chiral Gaussian ensemble with exponential decay (Ch-EE):** here the ensemble of  $C$ -matrices corresponds to an exponential decay of the variances away from the diagonals  $C_{kk}$  but with mean  $\langle C_{kl} \rangle = 0$  for all  $k, l$ . The  $\rho(H)$  is again given by eq.(4) with

$$h_{kl} = \langle C_{kl}^2 \rangle = \exp \left( -\frac{|k-l|}{b} \right)^2, \quad b_{kl} = \langle C_{kl} \rangle = 0 \quad \forall k, l \quad (26)$$

with  $b$  as an arbitrary parameter. Eq.(6) now gives

$$Y = -\frac{1}{2M\gamma} \left[ 2 \sum_{r=0}^N (N-r) \ln \left( 1 - \frac{2\gamma}{\exp(\frac{r}{b})^2} \right)^2 \right] + c_0 \quad (27)$$

with  $M = N^2$  and  $r \equiv |k-l|$ .

To keep analogy with the other ensembles described above, here again the initial ensemble for  $C$  is chosen that of the diagonal matrices with a Poisson spectral statistics which corresponds to  $Y_0 = c_0$ . Referring localization length as  $\xi$  and using  $\Delta_e(e) = \frac{2N}{\xi} \Delta(e)$ , the spectral complexity parameter now becomes

$$\Lambda_{e,E}(b, e) = \frac{\xi^2 R_1^2}{8\gamma N^4} \left[ 2 \sum_{r=0}^N (N-r) \ln \left( 1 - \frac{2\gamma}{\exp(\frac{r}{b})^2} \right)^2 \right] \quad (28)$$

For numerics, here again we consider an ensemble of 5000 matrices of size  $2N = 1000$  and another of 2500 of size  $2N = 2000$ ; both ensembles are analyzed for two  $b$ -values i.e  $b^2 = 50$  and  $100$ . Our analysis reveals that the approximation  $\xi \sim \langle I_2 \rangle^{-1}$  is not valid for this case but taking  $\xi \approx \sqrt{2N}$  gives results consistent with our theoretical claim about  $\Lambda_e$ . More clearly, the numerical analysis confirms analogy of the spectral measures of a Ch-EE with

parameter  $b = b_1$  and at energy  $e = e_1$  with another Ch-EE at  $b = b_2$  and energy  $e = e_2$  i.e if  $\Lambda_{e,E}(b_1, e_1) = \Lambda_{e,E}(b_2, e_2)$  (note, in general,  $b_1 \neq b_2, e_1 \neq e_2$ ).

## B. Numerical Analysis

A comparison of the spectral fluctuations for different complex systems in general requires a prior rescaling of the spectrum by the local mean level spacing (referred as unfolding). But for systems where the density of states is not a smooth function of energy (as in the chiral spectrum near  $e = 0$ ), the unfolding procedure becomes nontrivial. Further as the statistics for non-stationary ensembles depends on  $\Delta_{loc}$  even after unfolding (through its dependence on  $\Lambda_e$ ), it changes rapidly in the regions with sharp change of  $\Delta_{loc}$ . As a consequence, it is numerically difficult to consider a spectral range with an appropriate number of levels without mixing of different statistics. To overcome this difficulty, here we consider nearest neighbour spacing ratio distribution  $P(r) = \sum_{i=1}^{N-1} \langle \delta(r - r_i) \rangle$  for spectral analysis, with the ratio  $r$  defined as the ratio of consecutive spacings between nearest neighbor levels:  $r_i = s_{i+1}/s_i$  where  $s_i = e_{i+1} - e_i$  is the distance between two nearest neighbour eigenvalues [29, 30]. For the spectral statistics in Poisson and Wigner-Dyson limit,  $P(r)$  can be given as

$$P(r) = \frac{c_\beta (r + r^2)^\beta}{(1 + r + r^2)^{1+(3/2)\beta}} \quad \text{Wigner - Dyson} \quad (29)$$

$$= \frac{1}{(1 + r)^2} \quad \text{Poisson} \quad (30)$$

with  $c_1 = \frac{27}{8}$  and  $c_2 = \frac{81\sqrt{3}}{4\pi}$ . As the ratio  $r_i$  does not depend on the local density of states, the unfolding of spectrum for  $P(r)$  is not required. Further  $P(r)$  being a short range fluctuation measure, it reduces the chances of mixing spectral statistics.

A  $\Lambda_e$  based comparison of the spectral fluctuations in general requires a prior knowledge of  $R_1(e)$  as well as ensemble averaged localization length. As mentioned above, for some cases, the latter can be estimated from the average inverse participation ratio  $\langle I_2 \rangle$ . In absence of a theoretical formulation of these measures, an option left to us is to derive the relevant information by a numerical analysis. Figures 1 and 2 illustrate the energy as well as system dependence of  $F(e) = R_1(e)/2N$  and  $\langle I_2 \rangle$ , respectively, for four ensembles. Although  $\langle I_2 \rangle$  results for Ch-BE and Ch-EE do not enter in our  $\Lambda_e$  calculations for these case, but their behavior is displayed in the figure for comparison with other two cases. Using  $F(e)$  and  $\langle I_2 \rangle$

(latter only for Ch-AE and Ch-PE) at a given  $e$  from these figures, we calculate  $\Lambda(e)$  for the four ensembles.

As clear from eqs.(19, 22, 25, 28),  $\Lambda_e$  for each ensemble not only depends on the energy-range  $e$  of interest but also on at least two other system-parameters. The analogy of the local spectral statistics among the ensembles can then manifest in many ways. More clearly, if indeed governed by  $\Lambda_e$  only as predicted by our theory, an analogy for the local correlations compared at different energies can occur within the same ensemble but by varying other distribution parameters. For example if  $\Lambda_{e,x}(s_1) = \Lambda_{e,x}(s_2)$  with  $x = B, A, P, E$  and  $s_1, s_2$  referring to two different sets of parameters for a specific " $x$ ", the local correlations at  $s_1, s_2$  are expected to be equal; this is later on referred as the "intra-system" analogy. Similarly if  $\Lambda_e$  at a specific energy  $e$  for different ensembles are equal, their local correlations at that energy should be analogous too. For example if  $\Lambda_{e,x}(e) = \Lambda_{e,y}(e)$  with  $x, y = B, A, P, E$ , the local correlations for the ensemble  $x$  at  $e$  are then predicted to be analogous to that of  $y$ ; (later referred as the "inter-system" analogy).

To confirm our theoretical prediction, here we numerically verify both these analogies by comparing the distribution of spacing ratio for a number of combinations, predicted to be the local spectral analogues. The details are as follows.

**Intra-system analogy:** The system parameters for the analogs can be obtained by invoking following condition

$$\Lambda_{s_1,x} = \Lambda_{s_2,x} = \Lambda_{s_3,x} = \Lambda_{s_4,x}. \quad (31)$$

with  $\Lambda_{e,x}$  is given by eq.(19), eq.(22), eq.(25) and eq.(28) for  $x = B, A, P, E$  respectively.

Fig 3 displays a comparison of  $P(r)$  behavior for Ch-AE obtained from four different combinations of disorder  $w$  and system size  $N$  at a specific energy  $e$ . Here the parametric combinations are chosen such that eq.(31) is satisfied (with  $\gamma = 1/4$ ). To confirm the analogy for all  $\Lambda_e$  ranges, large or small, the comparison is considered for five different  $\Lambda_e$  values. To indicate that the statistics is indeed changing with  $\Lambda_e$ , the two stationary limits, namely,  $P(r)$  for Poisson and GOE cases (eqs.(29, 30)) are also displayed in each part of the figure. Similar fig 4-6 show  $P(r)$  for four different Ch-BEs (obtained by changing  $\mu, N, e$ ), Ch-PEs (different combinations of  $b$  and size  $N$  and  $e$ ) and Ch-EEs (different combinations of  $b^2, N, e$ ) respectively. The figures reconfirm our theoretical prediction regarding the insensitivity of

local spectral statistics to specific system details and the role played by  $\Lambda_e$ .

**Inter-system analogy:** The condition for the system parameters leading to the analogs now becomes

$$\Lambda_{e,B} = \Lambda_{e,A} = \Lambda_{e,P} = \Lambda_{e,E} \quad (32)$$

with  $\Lambda_{e,B}$ ,  $\Lambda_{e,A}$ ,  $\Lambda_{e,P}$ ,  $\Lambda_{e,E}$  given by eq.(19), eq.(22), eq.(25) and eq.(28) respectively (with  $\gamma = 1/4$ ). As illustrated in Fig. 7,  $P(r)$  for all the four cases overlap with each other if their  $\Lambda_e$  are equal. The details of the each ensemble used in numerics is given in the figure 7.

**Analogy at  $e = 0$ :** The relevance of behavior near zero-energy modes in many studies of chiral systems motivates us to compare  $P(r)$  at energy  $e = 0$ . The comparison of the four ensembles at  $e = 0$ , while the condition (32) is fulfilled by varying other system parameters, is depicted in fig 8. The convergence of  $P(r)$  behavior for each case to the same curve reconfirms the predicted role of  $\Lambda_e$  in local spectral statistics. Further as a sudden increase in  $R_1(e)$  near  $e = 0$  implies a very large  $\Lambda_e$ , the statistics for each case is expected to approach the Ch-GOE limit (equivalently Wigner-Dyson limit for  $\beta = 1$  given by eq.(29). The expectation is also consistent with the display in figure 8; (the deviation seen from Ch-GOE arises due to averaging over a finite (although small) spectral range near  $e = 0$ ).

## V. CONNECTION TO OTHER COMPLEX SYSTEMS

As described below, the multi-parametric chiral ensembles are not only connected to Chiral Brownian ensembles but also to some other complex systems too. The results and insights in the statistics of any one of them have therefore important implications for the others.

### A. Multi-parametric Wishart ensembles

The appearance of Wishart matrices in wide ranging areas has already motivated many research studies on Wishart random matrix ensembles. Most of these studies are however confined to the domains of i.i.d matrix elements and not much information is available for sparse matrices or matrix elements with varying degree of the distribution. The present study fulfils this information gap as follows. Consider  $N \times N$  matrix  $L_1 \equiv C.C^\dagger$  and

$(N + \nu) \times (N + \nu)$  matrix  $L_2 \equiv C^\dagger.C$  with  $C$  same as in eq.(1). Both  $L_1$  and  $L_2$  correspond to Wishart matrices. The ensemble density  $\rho_c(C)$  given by eq.(3) then leads to multi-parametric ensemble densities, say  $\rho_{L_1}(L_1)$  and  $\rho_{L_2}(L_2)$ , of  $L_1$  and  $L_2$  respectively

$$\rho_{L_1}(L_1) = \int \delta(L_1 - C.C^\dagger) \rho_c(C) DC \quad (33)$$

$$\rho_{L_2}(L_2) = \int \delta(L_2 - C^\dagger.C) \rho_c(C) DC \quad (34)$$

Taking derivative of eqs.(33,34) and subsequent use of eq.(5) along with partial integration then leads to a complexity parametric governed diffusion for  $\rho_{L_1}(L_1)$  and  $\rho_{L_2}(L_2)$ ; their diffusion equations turned out to be analogous to those of Wishart Brownian ensembles (WBE) of  $L_1$  and  $L_2$ , discussed in [31]. The mapping then helps to determine the strength fluctuation measures for  $\rho_{L_1}(L_1)$  and  $\rho_{L_2}(L_2)$  from those of WBE; (the measures for WBE of  $L_1$  are discussed in [31]).

As the eigenvalues and eigenfunctions of  $L_1$  and  $L_2$  are closely related to those of  $H$ , the mapping mentioned above is also relevant to determine the strength measures for  $\rho(H)$ . This can be explained as follows: rewriting the eigenvector pair  $U_n, U_{n+N}$  of  $H$  corresponding to eigenvalue pair  $e_n, e_{n+N}$  as  $\begin{pmatrix} X_n \\ \pm Z_n \end{pmatrix}$  with  $X_n, Z_n$  as column vectors with  $N$  components and  $N + \nu$  components respectively, it is easy to see from eq.(1) that

$$C^\dagger C Z_n = \lambda_n Z_n, \quad C C^\dagger X_n = \lambda_n X_n. \quad (35)$$

where  $\lambda_n = e_n^2$ ,  $n = 1 \rightarrow N$  are non-zero eigenvalues of  $L_1$  and  $L_2$  corresponding to eigenfunctions  $X_n$  and  $Z_n$ , respectively. The information about the statistics of  $X_n$  and  $Z_n$  can then be used to determine that of  $U_n$ .

Further the JPDF  $P_\lambda(\lambda_1, \dots, \lambda_N)$  of the eigenvalues is related to JPDF  $P_s(e_1, e_2, \dots, e_N)$  of the singular values of  $C$  (with  $e_n$  as the singular eigenvalues of  $C$  or  $C^\dagger$ )

$$P_\lambda(\lambda_1, \dots, \lambda_N) = P_s(\sqrt{\lambda_1}, \sqrt{\lambda_2}, \dots, \sqrt{\lambda_N}) \prod_{n=1}^N (2\sqrt{\lambda_n}), \quad (36)$$

But, following pairwise degeneracy of the non-zero eigenvalues,  $P(E)$ , discussed in section III, is also related to  $P_s$

$$P(E) \equiv P_s(e_1, e_2, \dots, e_N) \prod_{k=1}^N \delta(e_k + e_{k+N}) \prod_{n=1}^{\nu} \delta(e_{2N+n}) \quad (37)$$

Clearly the spectral fluctuations of  $P(E)$  and  $P_\lambda$  are related and the information about one can be used for the other.



## B. Calogero-Sutherland Hamiltonian

As discussed in [25], the diffusion equation for  $P(E, Y)$  can be rewritten in terms of the Schrodinger equation  $\frac{\partial \Psi}{\partial Y} = \mathcal{H} \Psi$  for the general state  $\Psi(E, Y) = \frac{P(E, Y)}{|Q|^{\beta/2r}}$  of a variant of the Calogero-Sutherland (CS) Hamiltonian of the interacting particles (with eigenvalues now playing the role of particles):

$$\mathcal{H} = \sum_i \frac{\partial^2}{\partial e_i^2} - \frac{\beta(\beta - 2)}{2} \sum_{i,j;i \neq j} \frac{e_i^2 + e_j^2}{(e_i^2 - e_j^2)^2} + g_0 \sum_k \frac{1}{e_k^2} - \frac{\gamma^2}{4} \sum_i e_i^2 + c_0 \quad (38)$$

with  $c_0 = \frac{N}{2}(\alpha + 1)\gamma + \frac{\gamma}{2}\beta N(N - 1)$ ,  $g_0 = \frac{\alpha}{4}(2 - \alpha)$  and  $\alpha = \frac{\beta}{2}(1 + 2\nu)$ . The ground state and many of the excited states of the standard CSH (and many variants) have already been worked out and relevant information about its particle correlations is available. The information can then be used in deriving the solution for  $P(E, Y)$  and the spectral correlations for the present case. (A similar connection between circular Brownian ensembles and standard CSH has been used in past to derive the spectral correlations for the former [27]. Although, in the present case, the steps remain essentially same but the difference in confining potential is expected to manifest in long range correlations).

## VI. CONCLUSION

In the end, we summarize with a brief discussion of our main results and open questions. Extending the complexity parameter formulation for Hermitian ensembles without chirality to those with chirality, we derive, for the latter, the complexity parameter and the response of the eigenvalues and eigenfunctions to the multi-parametric variations. As the chiral cases include non-Hermitian matrix blocks, this not only renders the technical analysis more complicated but also lead to the diffusion equations for the spectral JPDF different from the case without chirality. But, as in the non-chiral case, the spectral complexity parameter in the chiral case is again a function of energy as well as ensemble parameters. This predicts an important connection hidden underneath the local spectral fluctuations of a complex system: its statistics at an energy for a given set of system condition can be analogous to that at another energy but with different system conditions. For two different complex systems, however, the analogy can occur even at same energy if their complexity parameters are equal and both belong to same global constraint class; (the latter ensures that both ensembles belong to same symmetry class and conservation laws). Our theoretical

predictions are confirmed by a numerical comparison of the spectral statistics of four multi-parametric Gaussian ensembles with different sets of ensemble parameters at a fixed energy and also for each ensemble at different energies. A similar comparison for the eigenfunction fluctuations is also very desirable.

Our study still leaves many questions unanswered. The first and foremost among them is a thorough analysis of the eigenfunctions correlations near zero mode. Another important question is about the transition from multi-parametric chiral ensembles to non-chiral ensembles as chiral symmetry is partially broken. We intend to pursue some of these studies elsewhere.

- 
- [1] A. Altland and M.R.Zirnbauer, Phys. Rev. B 55, 1142, (1997).
- [2] P. Shukla, Int. J. Mod. Phys. B (WSPC) 26, 12300008, (2012).
- [3] F.Dyson, J. Math. Phys. 3, 1191 (1962).
- [4] F. Haake, *Quantum Signatures of Chaos*, Springer (Berlin), (1991).
- [5] M. L. Mehta, *Random Matrices*, Academic Press, (1991).
- [6] T. Guhr, G. A. Muller-Groeling and H. A. Weidenmuller, Phys. Rep. 299, 189 (1998).
- [7] A. Ferreira and E.R.Mucciolo, Phys. Rev. Lett., 115, 106601, (2015); A. Cresti, F. Ortmann, T. Louvet, Dinh Van Tuan and S. Roche, Phys. Rev. Lett, 110, 196601 (2013); L. Liu, Y. Yu, H-B Wu, Y-Y Zhang, J-J Liu and S-S Li, Phys. Rev. B 97, 155302 (2018); N. Weik, J. Schindler, S. Bera, G.C. Solomon and F. Evers, Phys. Rev. B 94, 064204 (2016); Santhosh G., V. Sreenath, A. Lakshminarayan, and R. Narayanan, Phys. Rev. B 85, 054204 (2012); N. M. R. Peres, S-W Tsai, J. E. Santos and R. M. Ribeiro, Phys. Rev. B 79, 155442 (2009).
- [8] J.J.M. Verbaarschot, Phys. Rev. Lett. 72 (1994) 2531; J.J.M. Verbaarschot, Nucl. Phys. B (Proc. Suppl.) 53 (1997) 88; T. Wettig, A. Schafer, H.A. Weidenmuller, Nucl. Phys. A 610, 492c, (1996). J.J.M. Verbaarschot and T. Wettig, 2000, Annu. Rev. Nucl. Part. Sci. 50, 343.
- [9] R. Gade, Nucl. Phys. B398 (1993) 499.
- [10] K. Slevin and T. Nagao, Phys. Rev. Lett. 70, 635, (1993).
- [11] C. W. J. Beenakker, Rev. Mod. Phys., 87, 1037, (2015).
- [12] V. Gurarie and J.T. Chalker, Phys. Rev. B, 68, 134207, (2003).
- [13] S. N. Evangelou and D.E. Katsanos, J. Phys. A: Math. Gen. 36, 3237, (2003).
- [14] H.Schomereus, M. Marciani and C.W.J. Beenakker, Phys. Rev. Lett. 114, 166803, (2015).
- [15] P.Shukla, Phys. Rev. E, 62, 2098, (2000).
- [16] P. Shukla, J. Phys.: Condens. Matter 17, 1653 (2005).
- [17] P. Shukla, Phys Rev. E 71, 026226 (2005).
- [18] R. Dutta and P. Shukla, Phys. Rev. E 76, 051124 (2007).
- [19] P.Shukla, J.Phys. A, (2008).
- [20] P. Shukla, Phys. Rev. E 75, 051113 (2007)
- [21] S. Sadhukhan and P. Shukla, Phys. Rev. E, 96, 012109, (2017).
- [22] P.Shukla, New J. Phys. 18 (2016) 021004

- [23] J.B. French, V.K.B. Kota, A. Pandey and S. Tomsovic, *Ann. Phys.*, (N.Y.) 181, 198 and 235 (1988).
- [24] S. Kumar and A. Pandey, *Ann. Phys.* 326, 1877, (2011); *Phys. Rev. E*, 79, 026211, (2009).
- [25] P.Shukla, preprint.
- [26] P. Shukla, *AIP conf. Proc.* 553, 215 (2001).
- [27] A. Pandey and P. Shukla, *J. Phys. A*, 24, 3907, (1991).
- [28] Antonio M. García-García and K. Takahashi, *Nucl.Phys.* B700 (2004) 361.
- [29] V. Oganesyan and D.A.Huse, *Phys. Rev. B* 75, 155111, (2007).
- [30] Y.Y. Atas, E. Bogomolny, O. Giraud and G. Roux, *Phys. Rev. Lett.* 110, 084101, (2013).
- [31] P. Shukla, *J. Phys. A: Math. Theor* 50, 435003 (2017)

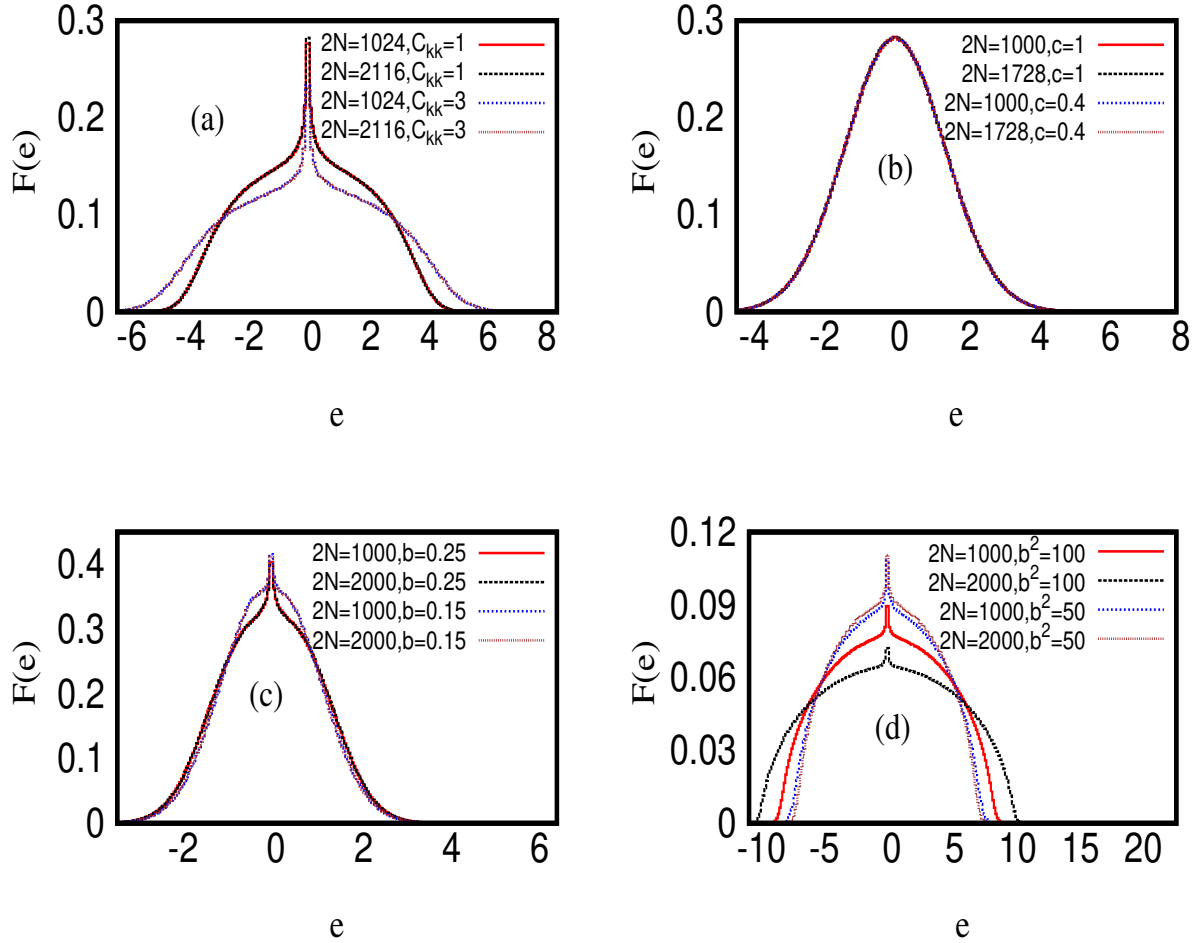


FIG. 1. **Density of states:** The determination of spectral complexity parameter  $\Lambda_e$  requires a prior knowledge of the ensemble averaged level density. The parts (a),(b),(c), (d) display the scaled level-density  $F(e) = R_1(e)/2N$  for the cases Ch-AE, Ch-BE, Ch-PE and Ch-EE respectively. As clear from the parts (a) and (c), Ch-AE and Ch-PE show a strong dependence of  $F(e)$  on the variances  $h_{kl}$  of the matrix elements but insensitivity to the matrix size  $N$ . On the contrary, part (b) for Ch-BE indicates an independence of  $F(e)$  from  $h_{kl}$  while part (d) reveals its dependence on both  $h_{kl}$  as well as  $N$ ; the change in  $F(e)$  is however insignificant when the variance is small.

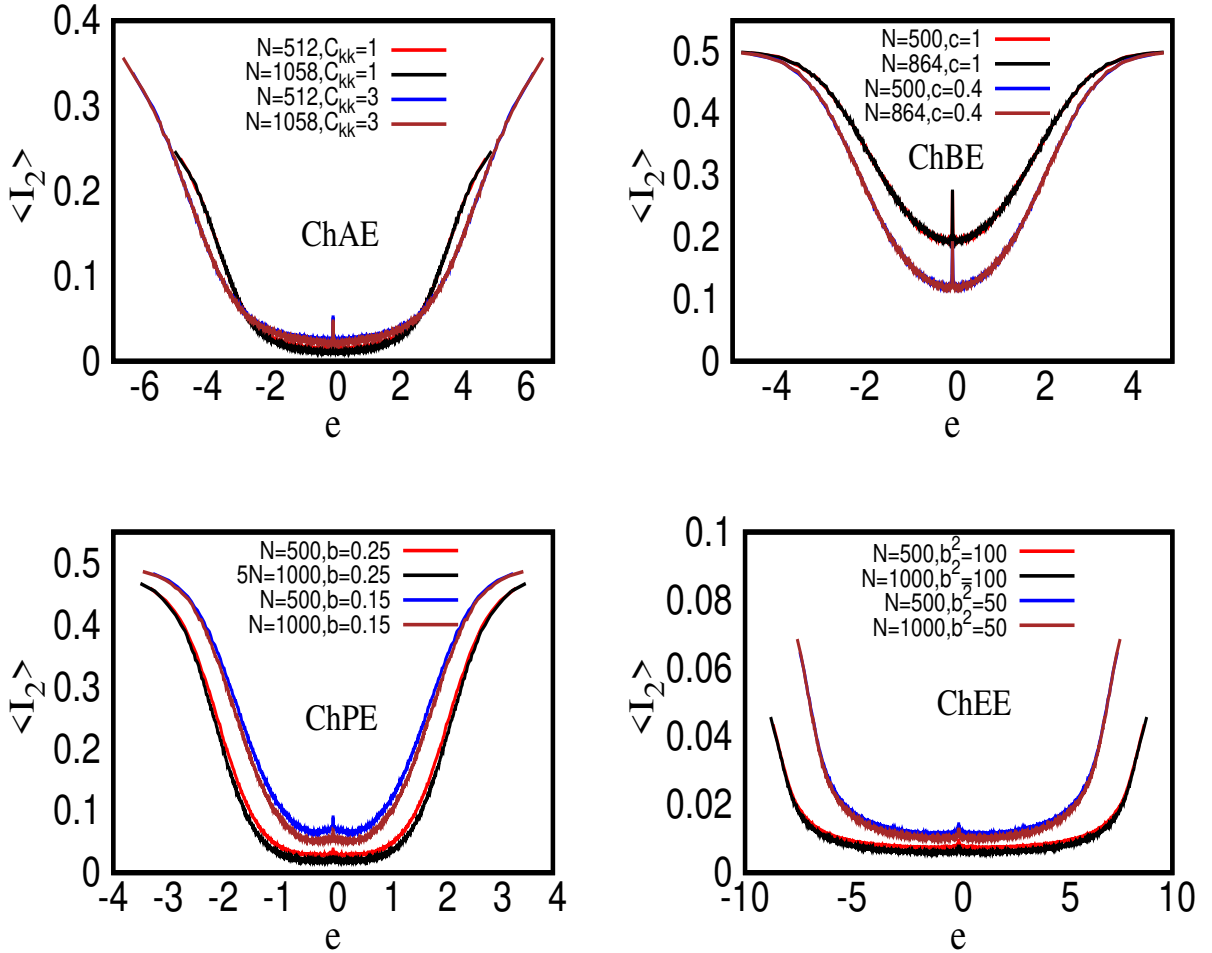


FIG. 2. **Ensemble averaged inverse participation ratio:** As mentioned in the text, a prior knowledge of the ensemble averaged  $\langle I_2 \rangle$  is needed to determine  $\Lambda_e$  for some cases ; the behavior for Ch-AE, Ch-BE, Ch-PE and Ch-EE is illustrated in parts(a),(b),(c),(d) respectively. As the parts (a) and (c) indicate,  $\langle I_2 \rangle$  for Ch-AE and Ch-PE is sensitive to the variance of the matrix elements but not to the matrix sizes  $N$ .

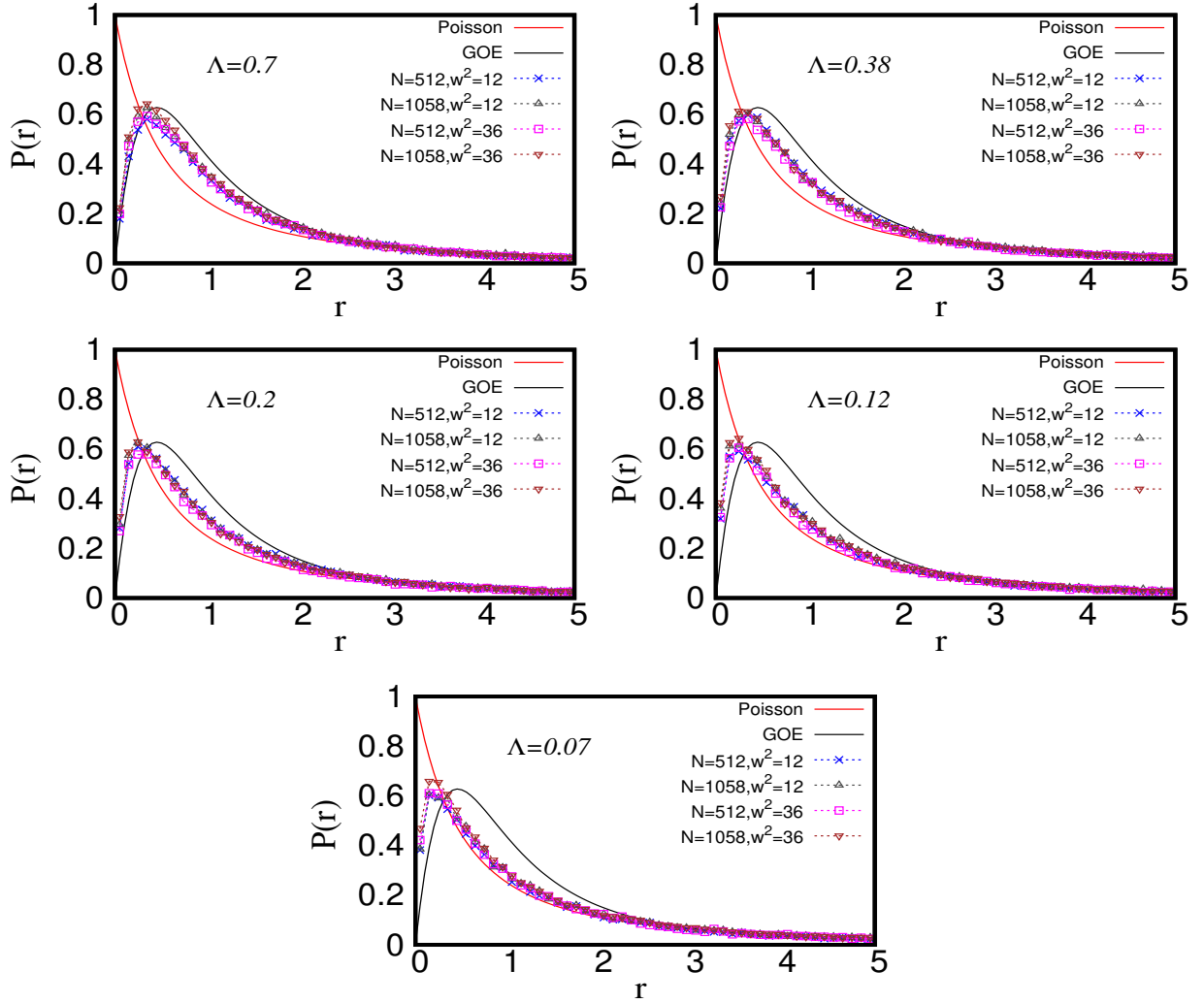


FIG. 3. **Intra-system analogy: nearest neighbour spacing ratio distribution for Ch-AE:**

As  $\Lambda_e$  for Ch-AE depends on the three system parameters  $e, w$  and  $N$ , their different combinations can result in same  $\Lambda_e$  value. (see eq.(31)) The figure here displays the analogies for five different  $\Lambda_e$ -values, latter spanning from Poisson ( $\Lambda_e \rightarrow 0$  to Ch-GOE ( $\Lambda_e \rightarrow \infty$ ) type spectral statistics. Each part of the figure displays the  $P(r)$  behavior for different Ch-AEs, corresponding to four different combinations of  $e, w, N$  which however keep their  $\Lambda_e$  equal. The theoretical limits of Poisson ( $\Lambda_e = 0$ ) and GOE ( $\Lambda_e = \infty$ ) is also shown for comparison. The convergence of  $P(r)$  for each case to the same curve and for all values of  $\Lambda_e$  lends support to our theoretical prediction about the latter being the only parameter governing the spectral fluctuations.

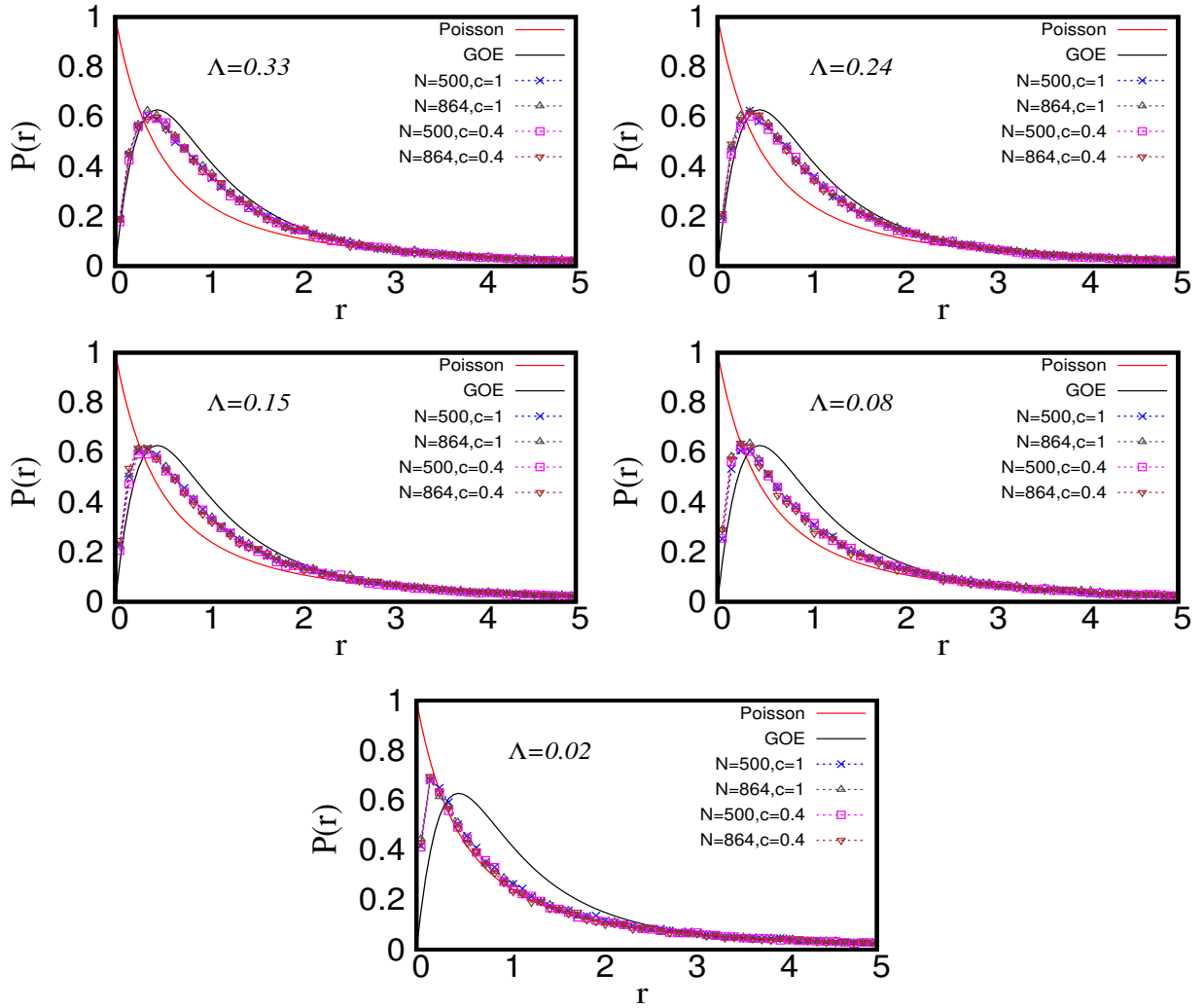


FIG. 4. Intra-system analogy: nearest neighbour spacing ratio distribution for Ch-BE: The details here are same as in figure 3 but now only two parameters namely  $c, N$  are available to achieve same  $\Lambda_e$ -value for different ch-BEs.



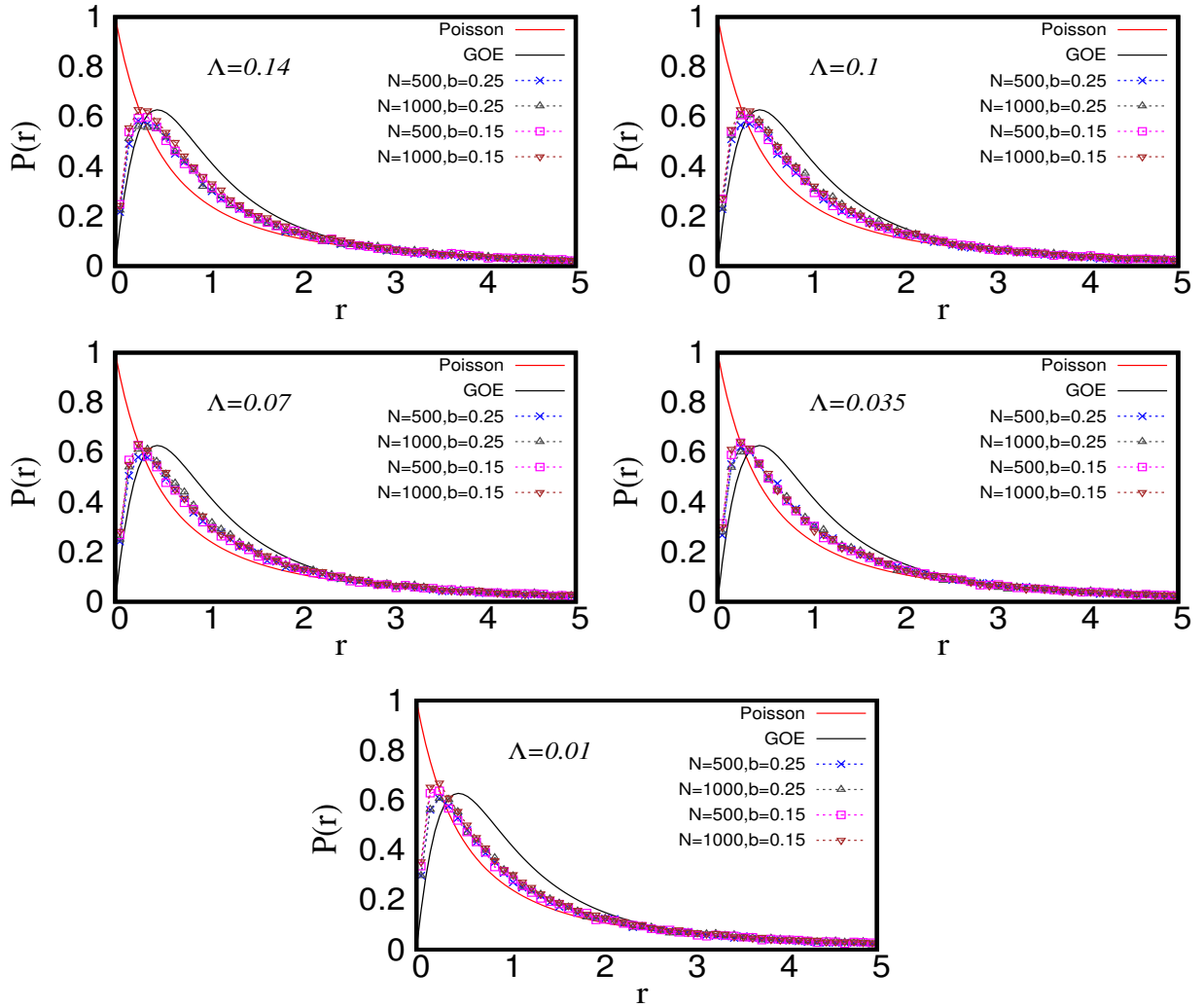


FIG. 5. Intra-system analogy: nearest neighbour spacing ratio distribution for Ch-PE: same as in figure 3 but here again only two parameters namely  $b, N$  are available to achieve same  $\Lambda_e$ -value for different ch-PEs.

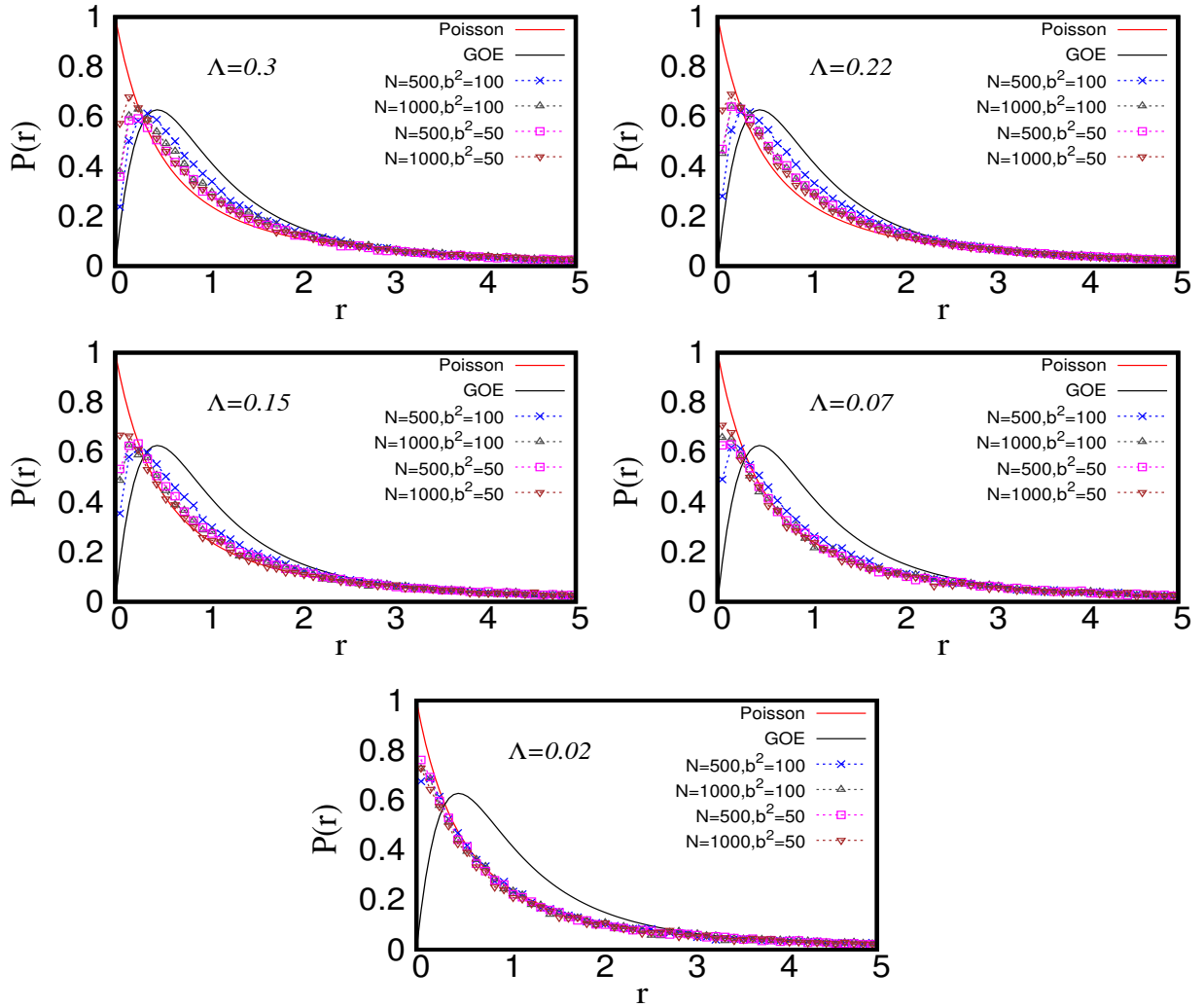


FIG. 6. Intra-system analogy: nearest neighbour spacing ratio distribution for Ch-EE: same as in figure 3 but here again only two parameters namely  $b, N$  are available to achieve same  $\Lambda_e$ -value for different Ch-EEs.

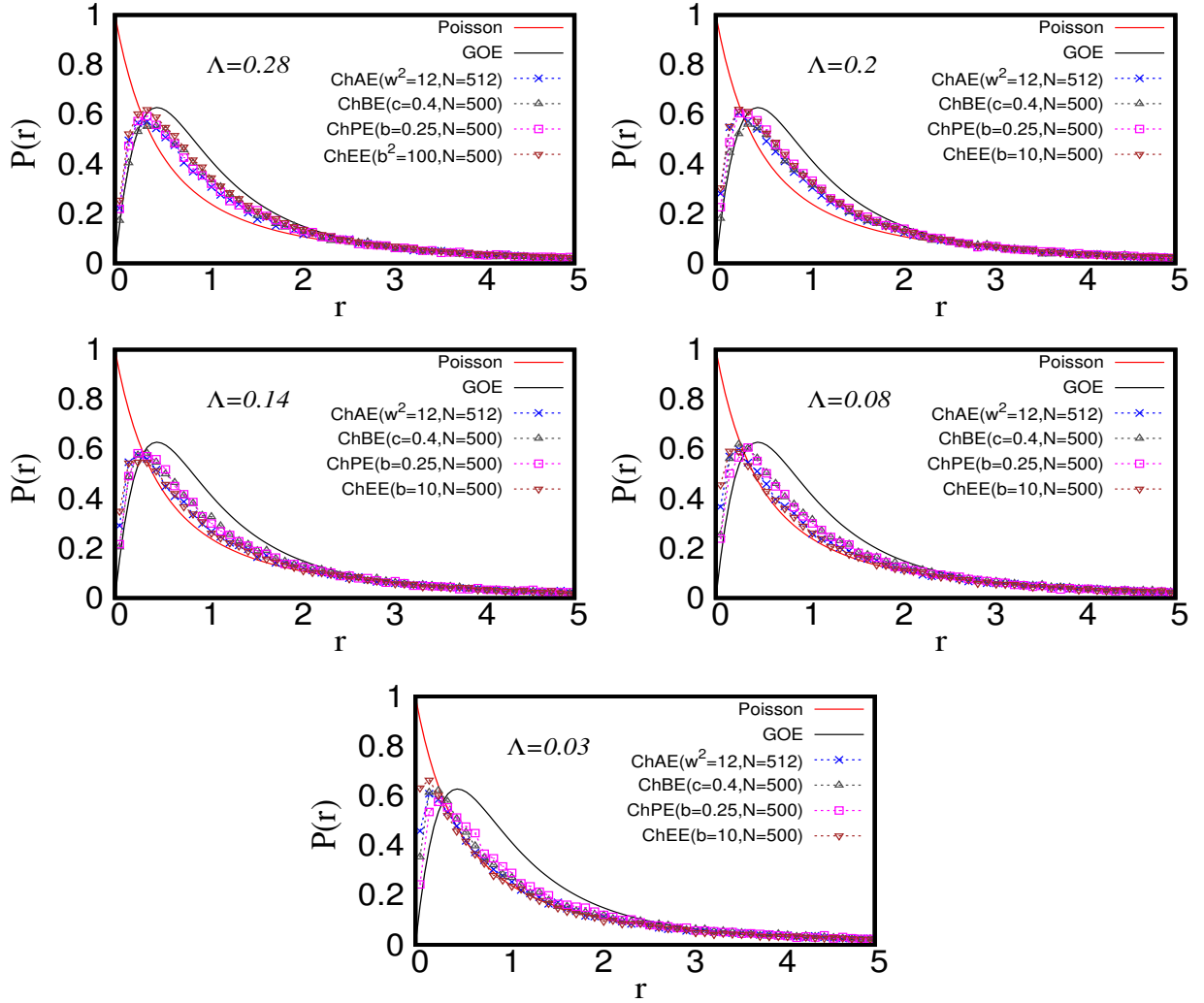


FIG. 7. **Inter system analogy: nearest neighbour spacing ratio distribution:** The figure displays the comparison of  $P(r)$  for four different ensembles, namely, ch-AE, ch-BE, ch-PE and ch-EE. Using eq.(22,19,25, 28), respectively, the system parameters in each case are chosen such that they lead to same  $\Lambda_e$  (see eq.(32)). The convergence of  $P(r)$  in each case to the same curve once again confirms the insensitivity of the spectral fluctuations to microscopic system details.

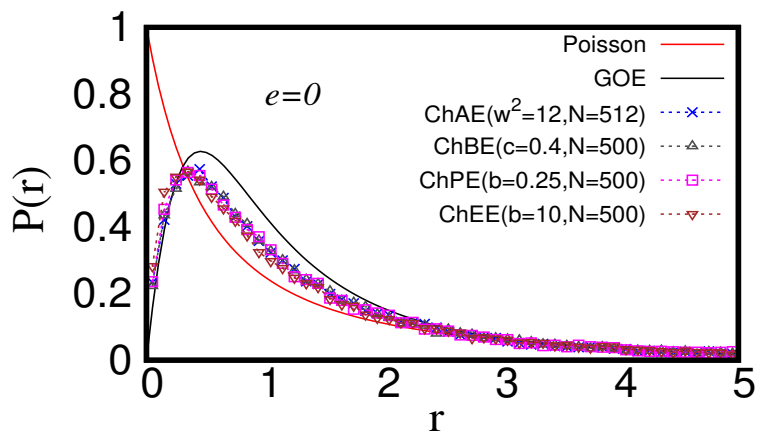


FIG. 8. **Nearest neighbour spacing ratio distribution at  $e = 0$ :** As in figure 7, here again we compare the four ensembles but now  $P(r)$  for each case is analyzed near  $e = 0$ . The details of the system parameters for each case are as follows: (i) Ch-AE:  $2N = 1024$ ,  $C_{ii} = 1$ , (ii) Ch-BE:  $2N = 1000$ ,  $c = 0.4$ , (iii) Ch-PE:  $2N = 1000$ ,  $b = 0.25$ , (iv) Ch-EE:  $2N = 1000$ ,  $b = 10$

. Clearly, as expected, the theoretical claim about  $\Lambda_e$  remains valid near zero mode too.